Regular Article

PLATELETS AND THROMBOPOIESIS

Interaction of platelet-derived autotaxin with tumor integrin $\alpha_V\beta_3$ controls metastasis of breast cancer cells to bone

Raphael Leblanc,[1] Sue-Chin Lee,[2] Marion David,[3] Jean-Claude Bordet,[4] Derek D. Norman,[2] Renukadevi Patil,[5] Duane Miller,[5] Debashish Sahay,[1] Johnny Ribeiro,[1] Philippe Clézardin,[1] Gabor J. Tigyi,[2] and Olivier Peyruchaud[1]

[1]Institut National de la Santé et de la Recherche Médicale, Unité Mixte de Recherche 1033, Université Claude Bernard Lyon 1, Faculté de Médecine Lyon Est, Lyon, France; [2]Department of Physiology, University of Tennessee Health Science Center, Memphis, TN; [3]Institut National de la Santé et de la Recherche Médicale, Unité Mixte de Recherche 1037, Université de Toulouse III, Institut Claudius Regaud, Toulouse, France; [4]EA4174, Université Claude Bernard Lyon 1, Faculté de Médecine Lyon Est, Lyon, France; and [5]Department of Pharmaceutical Sciences, University of Tennessee Health Science Center, Memphis, TN

Key Points

- ATX stored in α-granules of resting platelets is secreted upon tumor cell-induced aggregation leading to prometastatic LPA production.
- Nontumoral ATX promotes early bone colonization by breast cancer cells and contributes to the progression of skeletal metastases.

Autotaxin (ATX), through its lysophospholipase D activity controls physiological levels of lysophosphatidic acid (LPA) in blood. ATX is overexpressed in multiple types of cancers, and together with LPA generated during platelet activation promotes skeletal metastasis of breast cancer. However, the pathophysiological sequelae of regulated interactions between circulating LPA, ATX, and platelets remain undefined in cancer. In this study, we show that ATX is stored in α-granules of resting human platelets and released upon tumor cell-induced platelet aggregation, leading to the production of LPA. Our in vitro and in vivo experiments using human breast cancer cells that do not express ATX (MDA-MB-231 and MDA-B02) demonstrate that nontumoral ATX controls the early stage of bone colonization by tumor cells. Moreover, expression of a dominant negative integrin $\alpha_v\beta_3$-Δ744 or treatment with the anti-human $\alpha_v\beta_3$ monoclonal antibody LM609, completely abolished binding of ATX to tumor cells, demonstrating the requirement of a fully active integrin $\alpha_v\beta_3$ in this process. The present results establish a new mechanism for platelet contribution to LPA-dependent metastasis of breast cancer cells, and demonstrate the therapeutic potential of disrupting the binding of nontumor-derived ATX with the tumor cells for the prevention of metastasis. (*Blood*. 2014;124(20):3141-3150)

Introduction

Blood platelets play an essential role in cancer metastasis.[1-4] Metastatic breast cancer cells activate platelet aggregation and the production of the prometastatic bioactive lipid mediator, lysophosphatidic acid (LPA).[5] LPA exhibits growth factor-like activities via the promotion of cell proliferation, motility, invasion, and survival of both normal and neoplastic cells.[6] LPA activates a series of six G-protein–coupled receptors (LPA_1 to LPA_6) that mediate the pleiotropic actions of LPA and its effect on cancer progression and metastasis.[7] We have previously shown that LPA generated in the course of platelet activation controlled bone metastasis of breast cancer cells by stimulating tumor cell proliferation and secretion of pro-osteoclastic cytokines via LPA_1.[8] However, the molecular mechanisms of how tumor cells induce the production of LPA by platelets are not defined yet.

Autotaxin (ATX, ENPP2) is a unique member of the nucleotide pyrophosphate-pyrophosphatases family with lysophospholipase D activity catalyzing the production of LPA from lysophospholipid precursors, including lysophosphatidylcholine (LPC). ATX is physiologically present in blood, and *Enpp2* deficiency in mice leads to embryonic lethality due to vascular developmental defects. Heterozygous *Enpp2*$^{WT/-}$ knockout mice are healthy, but contain half the concentration of LPA in plasma compared with wild-type (WT) animals, demonstrating that ATX activity is the main source of LPA in the blood. However, the pathophysiological functions of circulating ATX and LPA remain elusive.

ATX was originally identified as an autocrine motility factor secreted by human A2058 melanoma cells.[9] Expression of ATX messenger RNA (mRNA) is consistently increased in primary tumors of multiple cancers compared with normal tissues, suggesting the involvement of ATX in oncogenesis and tumor progression.[10] Additionally, ATX expression has been shown to confer resistance to cancer chemotherapy and radiotherapy.[11] In the context of breast cancer, transgenic mice overexpressing ATX in the mammary gland develop spontaneous breast tumors and distant metastases, further supporting a role of ATX in tumorigenesis, invasion, and metastasis.[12] In animal models, we have shown that overexpression of ATX in breast cancer cells increased the rate of spontaneous lung and micromedullary bone marrow metastasis formation compared with ATX nonexpressing tumor cells.[13] Moreover, we have demonstrated that high ATX expression confers a selective advantage

Submitted April 8, 2014; accepted September 15, 2014. Prepublished online as *Blood* First Edition paper, October 2, 2014; DOI 10.1182/blood-2014-04-568683.

G.J.T. and O.P. contributed equally to this study.

The online version of this article contains a data supplement.

The publication costs of this article were defrayed in part by page charge payment. Therefore, and solely to indicate this fact, this article is hereby marked "advertisement" in accordance with 18 USC section 1734.

in the progression of osteolytic bone lesions.[13] However, ATX mRNA expression level in biopsies of human primary breast tumors does not predict metastasis recurrence or overall survival.[13] This observation suggests that expression of ATX at the primary tumor sites is not a suitable predictive biomarker of breast cancer metastasis.

Our present study demonstrates that ATX is taken up and stored in platelet α-granules and released upon tumor cell-induced platelet activation, leading to the production of LPA, and reveals for the first time, that nontumoral ATX (NT-ATX) controls the early stage of bone colonization by tumor cells.

Materials and methods

Cell culture and reagents

CHO-dhfr$^+$, CHOβ3WT, and CHOβ3-Δ744 cells and culture conditions were described previously.[14,15] Human cell lines from breast cancer (MDA-MB-231, MCF-7, ZR7-51, BT474, SKBr3, Hs578T, and T47D), prostate cancer (PC-3 and DU145), and osteosarcoma (MG63) were obtained from and cultured as recommended by American Type Culture Collection (Gaithersburg, MD). Characterization of MDA-MB-231/B02 (MDA-B02) and MDA-B02/luc breast cancer cells and culture conditions were described previously.[16,17] Human umbilical vein endothelial cells (HUVEC) were purchased from VEC Technologies (Rensselaer, NY). Construction and purification of recombinant ATX, as well as details for chemicals, reagents, and antibodies used are described in supplemental Materials and methods, available on the *Blood* Web site.

Preparation of human platelets and LPA quantification

Human blood was collected on acid citrate dextrose from healthy volunteers after informed consent, in accordance with the Declaration of Helsinki. Washed platelets were prepared as described previously.[5] The methods used for LPA quantification are described in supplemental Materials and methods.

Immunodetection assays

The methods used for cell surface detection of integrins, protein detection by western blotting and immunoprecipitation, and details for immunogold electron microscopy of ATX are presented in supplemental Materials and methods.

Reverse transcription-polymerase chain reaction (RT-PCR)

Total RNA extraction and cDNA synthesis were performed as previously described.[13] Expression of LPA G protein-coupled receptor was quantified by real-time quantitative RT-PCR (qRT-PCR) using gene-specific PCR primers in conditions detailed in supplemental Materials and methods.

Cell adhesion assays

Cell adhesion assays were done as previously described.[15] Plates were coated with bovine serum albumin (BSA), recombinant ATX, osteopontin (OPN) (Sigma-Aldrich), or fibronectin (FN) (Invitrogen). Cells were detached and resuspended in HEPES-Tyrode buffer supplemented with 2 mM Mn^{2+} (10^5 cells in 100 μL of buffer), rested for 1 hour at 37°C, and seeded on coated plates for 1 hour. Attached cells were fixed, stained with a solution of crystal violet, and counted under the microscope. Results were expressed as the number of attached cells per mm^2.

Cell proliferation assay

Cell proliferation assays induced by LPC (1 μM) were carried out as previously described.[18] MDA-B02 and MDA-MB-231 cell proliferation were conducted in presence of ATX (0.3 nM) and increasing concentrations of BMP22, and quantified by 5-bromo-2′-deoxyuridine incorporation. Platelet-induced tumor cell proliferation was carried out by seeding MDA-B02 cells (5×10^4 cells per well) in 96-well culture plates in Ham's F-12K medium (Life Technologies) containing endogenous Mg^{2+} (2.1 mM) without serum overnight. Washed human platelets (10^6/well) were added and incubated in Ham's F-12K medium in absence of serum and Mn^{2+} from 2 to 24 hours. Cells were fixed and stained with a solution of crystal violet, and proliferation was assessed by densitometry.

Cell invasion and transmigration assays

MDA-MB-231 cell invasion across a Matrigel layer coated onto 24-well BioCoat FluoroBlok tumor invasion system (8 μm-pore size; BD Biosciences) was performed as previously described.[13] Serum-free Dulbecco's modified Eagle medium/0.1% fatty acid-free–BSA supplemented with 0.1 nM recombinant ATX and 1 μM LPC 18:1, in presence or absence of the ATX inhibitor BMP22,[19] was used as chemoattractant. Cells that migrated to the bottom face of insert membranes were stained with Calcein-AM, and fluorescence cells were quantified using FlexStation 3 microplate reader (Molecular Devices, LLC). Transmigration assay through endothelial cell monolayer was conducted as previously described.[20] HUVEC cells (1×10^5, passages 4 to 7) in complete MCDB-131 medium were plated on cell culture inserts (8 μm pore size, polyethylene terephthalate membrane from BD Biosciences, Pharmingen) coated with 0.1% gelatin and incubated for 24 hours to form a monolayer. MDA-MB 231 cells were labeled with Calcein-AM and plated on the HUVEC monolayers. Serum-free MCDB-131/0.1% fatty acid-free–BSA medium, 0.75 mL/well with or without chemoattractant consisting of 0.1 nM recombinant ATX, and 1 μM 18:1 LPC was added to the bottom chamber. After 20 hours at 37°C, the number of MDA-MB-231 cells that invaded the HUVEC monolayer was counted using a fluorescence NIKON TiU inverted microscope.

Early bone colonization in breast cancer cell experiments

The animal protocol was reviewed and approved by the Institutional Animal Care and Use Committee of the Université Claude Bernard Lyon-1 (Lyon, France). Animals were purchased from Janvier Labs (Le Genest-Saint-Isle, France) and housed under closed barrier conditions as previously described.[13] MDA-B02/luc cells (5×10^5 in 100 μL of phosphate-buffered saline) were injected IV into the 4-week-old BALB/C nude mice as previously described.[17] Seven days postinjection, the mice were euthanized by cervical dislocation and the hind limbs were dissected. Bones were chopped and treated with 0.25 mg/mL collagenase for 2 hours at 37°C. The cell suspension was washed with phosphate-buffered saline and resuspended in complete media supplemented with 1 μg/mL puromycin. After 2 weeks, the clones were fixed and stained with a solution of crystal violet and counted.

Statistical analysis

Differences between groups were determined by 1-way or 2-way analysis of variance (ANOVA), followed by a Bonferroni posttest using GraphPad Prism v5.0c software. Single comparisons were carried out using the nonparametric Mann-Whitney *U* test. $P < .05$ was considered statistically significant.

Results

ATX is stored in α-granules of resting human platelets

First, we examined whether human platelets could be a source of ATX. Using qRT-PCR, we were unable to detect the expression of ATX mRNA in platelets from multiple donors (data not shown). Searching the Gene Expression Omnibus database,[21] we next examined ATX expression and found no evidence for ATX, fibrinogen α-chain, and immunoglobulin heavy chain (Figure 1A) in isolated megakaryocyte (MK) progenitors and in MKs expanded in vitro. The

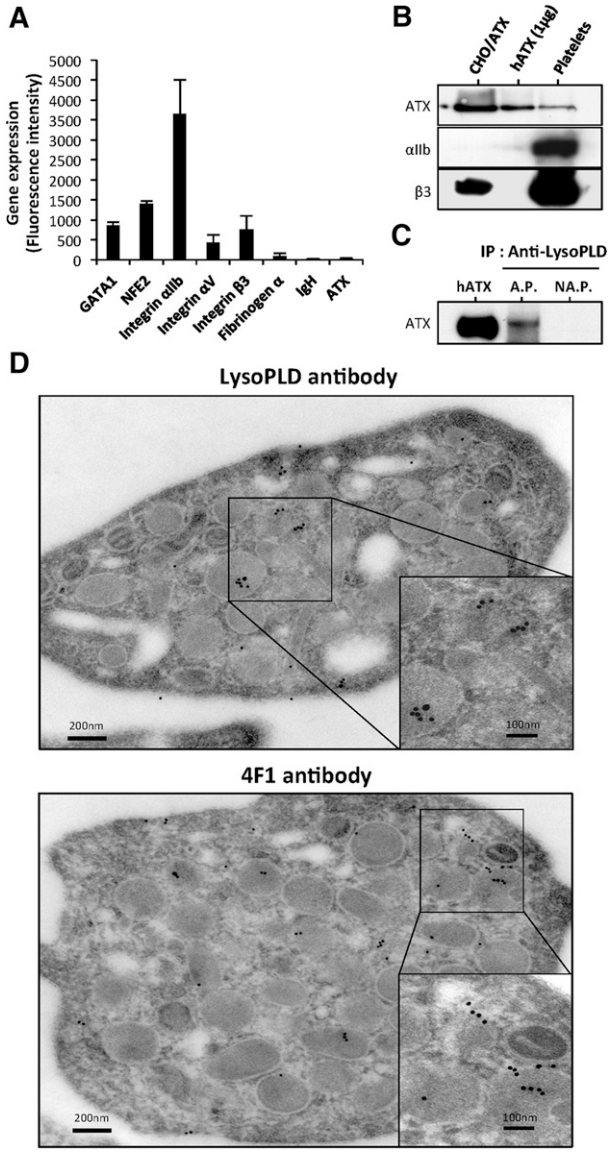

Figure 1. ATX is present in human platelets. (A) Gene expression in MKs. Mean of fluorescence intensity on Affymetrix MOE430A mouse array for GATA1, NFE2, integrin α_{IIb}, integrin α_V, integrin β_3, fibrinogen α-chain, immunoglobulin heavy chain, and ATX were calculated from GEO dataset accession numbers GSM152271 and GSM152272, as previously established.[21] (B) ATX expression in unstimulated human platelet lysate was detected by immunoblotting using anti-LysoPLD polyclonal antibody. Total CHO-dhfr+/ATX cell lysate and recombinant human ATX were used as controls. Integrin subunits α_{IIb} and β_3 were detected with specific antibodies. (C) Immunoprecipitation of ATX. Six releasates from aggregated platelets or supernatant from nonaggregated platelets were incubated with anti-LysoPLD antibody. ATX was immunodetected with the anti-LysoPLD antibody. (D) Image obtained from transmission electron microscopy of unstimulated human platelets. The grids were reacted with an anti-LysoPLD polyclonal antibody (top) or with 4F1 monoclonal antibody (bottom). The in situ localization of ATX was identified by gold particles after an amplification of the primary signal. AP, aggregated platelets; hATX, human ATX; NAP, nonaggregated platelets.

quality of mRNA was confirmed by high expression of transcription factors GATA1, NFE2, and integrin subunits α_{IIb}, α_V, and β_3 in our samples. Similar results were obtained with in vitro expanded MKs in the presence of thrombopoietin (data not shown), providing further evidence that MKs do not express ATX.

Platelets endocytose blood proteins independently of their activation state.[22] Because ATX is present in the blood circulation, we examined the hypothesis that plasma ATX could be taken up into platelets. ATX was detectable in the protein lysate of nonactivated, washed, human platelets by western blotting using an anti-lysoPLD

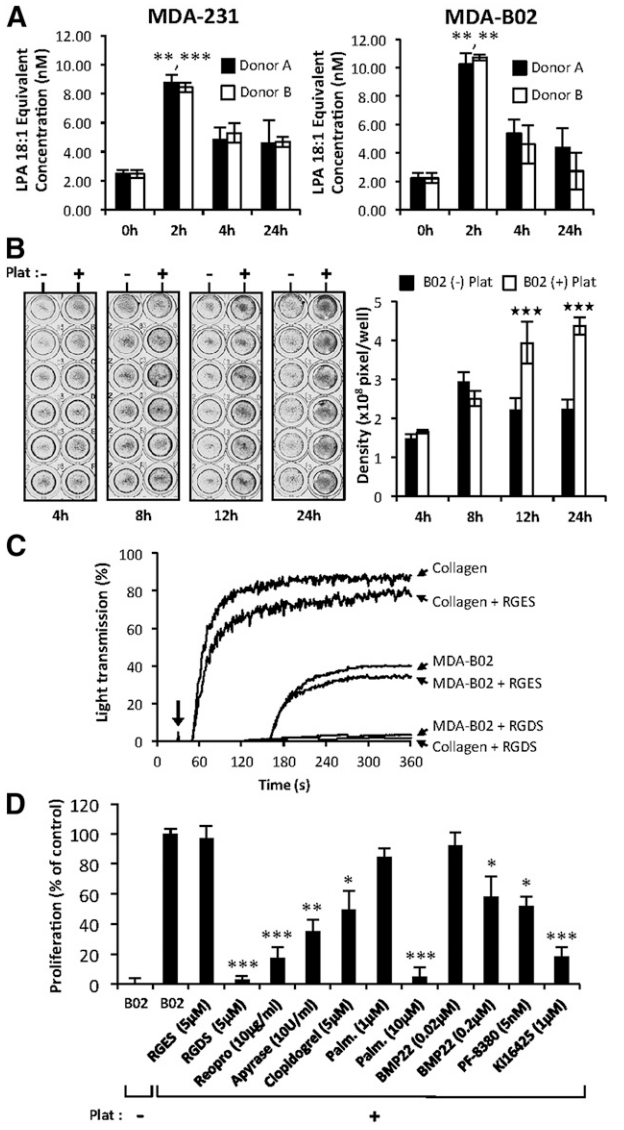

Figure 2. Tumor cells induced ATX secretion by platelets and the formation of bioactive LPA. (A) LPA production during passive coculture of breast cancer cells and human platelets. Adherent MDA-MB-231 (left) and MDA-B02 (right) cells were incubated for up to 24 hours in the presence of human platelets from 2 different donors. Data are expressed as mean fluorescence ratio value for each concentration, normalized to the percentage of LPA 18:1 response (**$P < .01$; ***$P < .001$; vs cancer cells at 0 hours using 1-way ANOVA with a Bonferroni posttest). (B) Adherent MDA-B02 cells were incubated in the presence (+) or absence (−) of human platelets in serum-free Ham's F-12K medium with endogenous Mg^{2+} (2.1 mM). Cell proliferation was assessed by densitometry analysis after cell staining with crystal violet (left). Data are expressed as mean density (± SD) of 6 replicates and are representative of 3 experiments (right). (***$P < .001$; vs MDA-BO2 (−) platelets using 2-way ANOVA with a Bonferroni posttest). (C) Platelet aggregation was stimulated by collagen (10 µg/mL) or by tumor cells (B02) (10^6 cells) at the time indicated by the arrow, in presence or absence of peptides. RGDS or RGES (100 µM) were added prior to the addition of collagen or tumor cells. Platelet aggregation was recorded over time as the percentage of light transmission. (D) Effects of inhibitors of platelet aggregation (RGDS, ReoPro, apyrase, and clopidogrel), phospholipase A1/2 activity (palmostatin B), lysoPLD activity (RG3-39 and PF-8380), and antagonist of $LPA_{1/3}$ receptor (Ki16425) on platelet-induced MDA-BO2 cell proliferation. MDA-BO2 cells were incubated for 12 hours in the presence (+) or absence (−) of human platelets. Culture media were supplemented with the indicated compounds. Data represent proliferation as the percentage of control (MDA-B02+Plat) (± SEM) of 6 replicates from 3 independent experiments (*$P < .05$; **$P < .01$; ***$P < .001$; vs MDA-BO2 (+) platelets using 1-way ANOVA with a Bonferroni posttest). Plat, platelets.

polyclonal antibody (Figure 1B). Additionally, we detected ATX in the releasate of type 1 collagen-induced platelet aggregation but not in the supernatant of nonaggregated platelets by immunoprecipitation using an anti-lysoPLD polyclonal antibody (Figure 1C). Moreover, a polyclonal and a monoclonal anti-ATX antibody for immunoelectron microscopy readily detected the presence of ATX in α-granules and sporadically in the open canalicular system of platelets (Figure 1D).

Cancer cells induce platelet activation and secretion of functionally active ATX and phospholipase A

Previous studies have shown that ATX binds platelet integrin $\alpha_{IIb}\beta_3$ contributing to thrombus formation and localizing LPA production.[23] Incubation of platelets with breast cancer cells in steering conditions induces LPA production.[5] In this study, we show that coincubation of platelets from 2 different donors with 2 different breast cancer cell lines in passive conditions induces a rapid increase in LPA concentration within 2 hours in the medium (Figure 2A). After 12 hours and 24 hours of coculture, a significant increase in MDA-B02 cell proliferation was observed compared with cultures grown in the absence of platelets (Figure 2B). To elucidate the role of integrin activation in platelet-induced tumor cell proliferation, we used selective inhibitors. The Arg-Gly-Asp-Ser (RGDS) peptide but not the Arg-Gly-Glu-Ser (RGES) control peptide blocked both collagen and tumor cell induced-platelet aggregation (Figure 2C). The RGDS peptide and ReoPro but not the RGES control peptide treatment blocked platelet-induced tumor cell proliferation, suggesting that platelet aggregation and activation of integrin $\alpha_{IIb}\beta_3$ were required in this process (Figure 2D). The requirement for platelet activation in platelet-induced tumor cell proliferation was further supported by the partial inhibition of tumor cell proliferation with inhibitors of the adenosine 5′-diphosphate activation pathway apyrase, and the P2Y12 inhibitor, clopidogrel (Figure 2D). The increase in platelet-induced cell proliferation was reduced by 80% ($P < .001$) with the $LPA_{1/3}$ receptor antagonist Ki16425, indicating that LPA produced by platelets in these coculture conditions was mediating the proliferative effect. To evaluate whether enzymes of the LPA production pathways were involved in platelet-induced tumor cell proliferation, we applied a nonspecific inhibitor of phospholipase A1/2 (palmostatin B) and 2 different ATX inhibitors (BMP22[19] and PF-8380[24]). Palmostatin B was as potent as the RGDS peptide in inhibiting platelet-induced tumor cell proliferation (Figure 2C). Both BMP22 and PF-8380 significantly inhibited tumor cell proliferation by 41% and 48%, respectively (Figure 2C). Altogether, these results reveal that interaction of cancer cells with platelets promotes platelet activation, and generation of LPA requires the sequential actions of phospholipase A1/2 followed by ATX.

Exogenous ATX controls breast cancer cell proliferation, invasion, and endothelial cell transmigration

In agreement with recent reports demonstrating that breast and prostate cancers have the lowest levels of ATX expression among many other cancer types,[25] we found that only the Hs578T breast carcinoma, MG63 osteosarcoma, and DU145 prostate cancer cells expressed ATX mRNA (Figure 3A). These results were in agreement with our previous findings showing that MDA-MB-231 and MDA-BO2 cells do not secrete ATX and are deprived of LPA production capacity as well.[5] Therefore, these cells that express predominantly LPA_1 as judged by real-time PCR analyses (Figure 3B), are ideal tools for investigating the role of NT-ATX in cancer cell dissemination. Proliferation of both cell lines was significantly

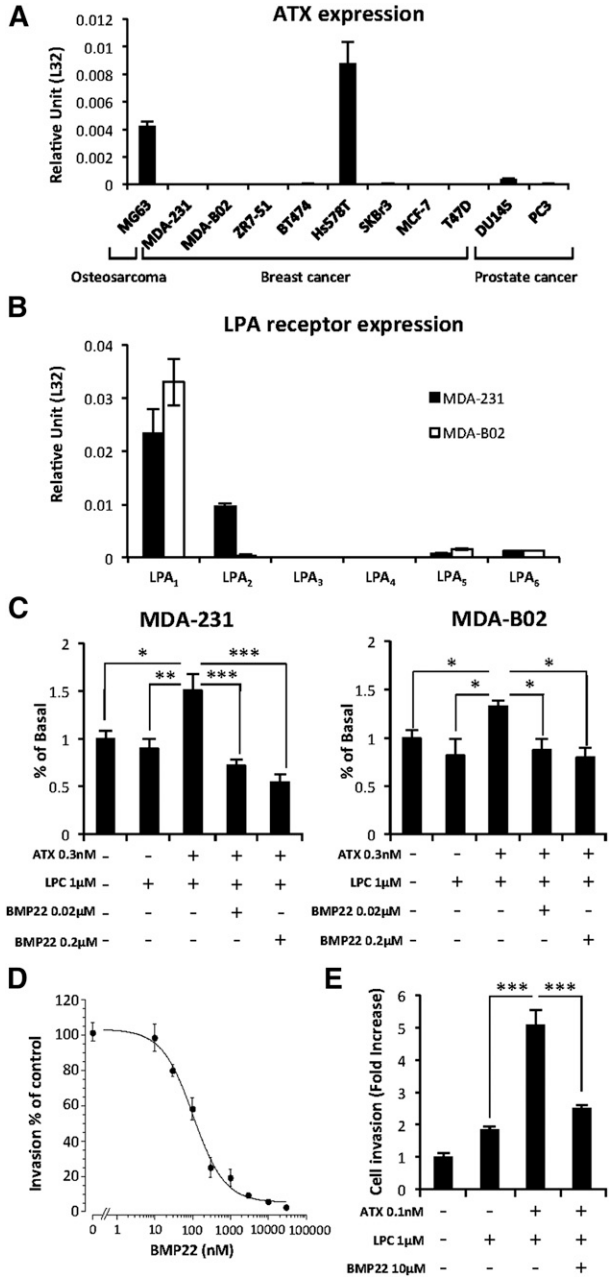

Figure 3. Exogenous ATX controls LPA-dependent cell proliferation and endothelial cell transmigration. (A) Real-time PCR analysis of ATX mRNA expression in osteosarcoma, breast, and prostate cancer cell lines. Values were normalized to housekeeping L32 gene. Data represent the mean (± SD) of 2 independent experiments performed in triplicate. (B) Real-time PCR analysis of LPA receptor ($LPA_{1\text{-}6}$) mRNA expression in MDA-231 and MDA-B02 cell lines. Values were normalized to housekeeping L32 gene. Data represent the mean (± SD) of 2 independent experiments performed in triplicate. (C) Cell proliferation assessed by 5-bromo-2′-deoxyuridine incorporation of MDA-MB-231 (left) and MDA-BO2 (right) cells in response to LPC and recombinant ATX in the presence or absence of BMP22. Results are expressed as the mean (± SD) of 3 independent experiments performed in 6 replicates (*$P < .05$; **$P < .01$; ***$P < .001$; vs cancer cells in presence of ATX and LPC using 1-way ANOVA with a Bonferroni posttest). (D) Effects of BMP22 on MDA-MB 231 cell invasion. Dose-response curves were generated in the presence of ATX and increasing concentrations of BMP22. Data represent the mean percentage of inhibition (± SEM) of 3 independent experiments performed in quadruplicate. (E) Effects of BMP22 on MDA-MB 231 cell transmigration across a HUVEC monolayer. Data represent the mean (± SEM) of 2 experiments performed in quadruplicate (***$P < .0001$ vs MDA-231 cells in presence of ATX and LPC using 1-way ANOVA with a Bonferroni posttest).

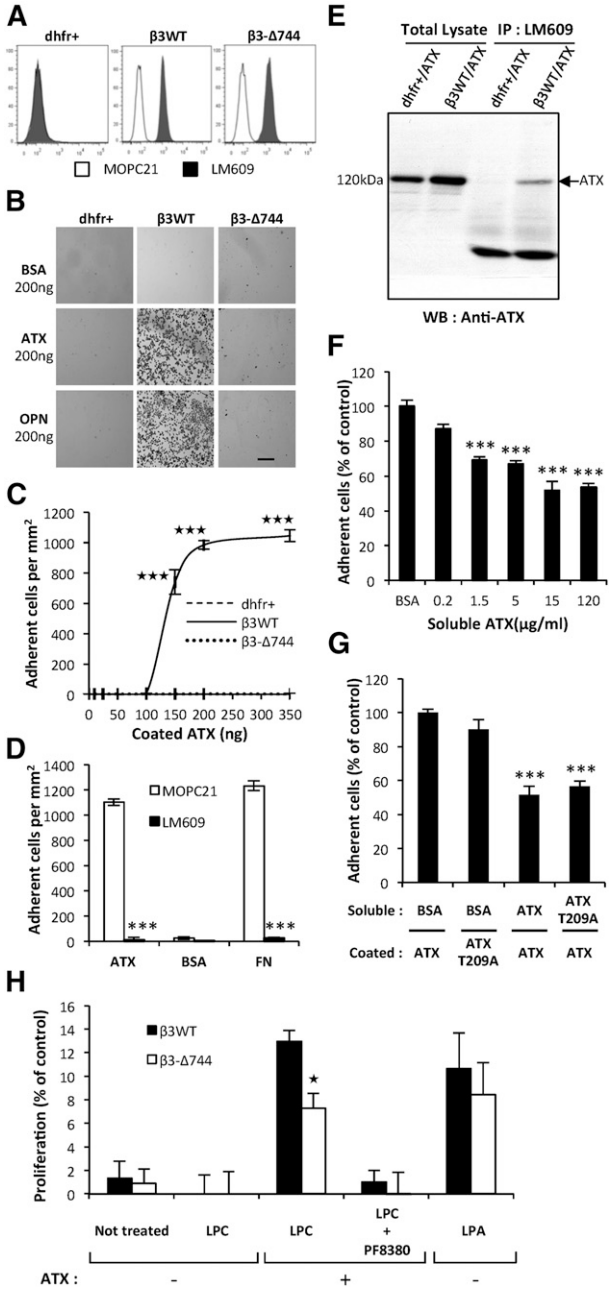

Figure 4. Functionally active integrin $\alpha_V\beta_3$ in cancer cells is required for ATX binding. (A) Flow cytometry detection of cell surface expression of integrin $\alpha_V\beta_3$ in parental CHO-dhfr$^+$ (dhfr$^+$, left), CHO-β_3WT (β3WT, middle), and CHO-β_3-Δ744 (β3-Δ744, right) cells. Cells were immunostained with the anti-human integrin $\alpha_V\beta_3$ monoclonal antibody, LM609 (dark histograms) or isotype control antibody, MOPC21 (open histograms). (B) CHO cell adhesion on ATX in presence of Mn^{2+} (2 mM). Optical microscopy observation of cell adhesion on ATX or OPN (scale bar: 200 μm). (C) Dose-response curves of cell adhesion were generated in the presence of increasing amounts of coated ATX. Data represent the mean of adherent cell/mm^2 (± SD) of 3 independent experiments performed in triplicate (***$P < .001$; vs CHO-dhfr$^+$ using 2-way ANOVA with a Bonferroni posttest). (D) Inhibition of CHO-β_3WT cell adhesion on ATX and FN with LM609 antibody. BSA was used as a negative control for cell adhesion. Cells were preincubated for 1 hour in the presence of LM609 or MOPC21 antibodies (10 μg/mL). Data represent the mean of adherent cell/mm^2 (± SD) of 3 experiments performed in triplicate (***$P < .001$; vs CHOβ_3WT cells treated with MOPC21 antibody using 1-way ANOVA with a Bonferroni posttest). (E) Coimmunoprecipitation of ATX and integrin β_3. Cell lysate from stable transfectants of CHO-dhfr$^+$/ATX and CHO-β_3WT/ATX expressing mouse ATX were incubated with LM609 antibody. ATX was immunodetected with the anti-LysoPLD antibody. (F) Soluble ATX inhibits cell adhesion of coated ATX. CHO-β_3WT cells were preincubated for 1 hour in the presence of soluble ATX (x-axis) prior to the adhesion assay. Data represent the mean percentage of adherent cells (± SEM) from 2 independent experiments performed in triplicate (***$P < .001$; vs CHOβ_3WT cells treated with BSA using 1-way ANOVA with a Bonferroni posttest). (G) Inhibition of CHO-β_3WT cell adhesion with soluble functionally active ATX or soluble lysoPLD-deficient ATX-T209A. Cells were preincubated for 1 hour in the presence of soluble ATX, soluble ATX-T209A, or BSA as control (15 μg/mL). Data represent mean percentage of adherent cells (± SD) of 2 experiments performed in triplicate (***$P < .001$; vs CHOβ_3WT cells treated with BSA using 1-way ANOVA with a Bonferroni posttest). (H) Cell proliferation of CHO-β_3WT (β3WT) and CHO-β_3-Δ744 (β3-Δ744) cells in response to LPC (1 μM) and recombinant ATX (1 nM), in presence or absence of PF8330 (5 nM) or in response to LPA (1 μM) in serum-free Ham's F-12K medium. Cell proliferation was assessed by densitometry analysis after cell staining with crystal violet. Data are expressed as mean density (± SD) of 6 replicates and are representative of 3 experiments. (*$P < .05$; vs CHO-β_3WT using 2-way ANOVA with a Bonferroni posttest).

enhanced in the presence of exogenous recombinant ATX and LPC (1 μM) that was specifically blocked by the ATX inhibitor BMP22 (Figure 3C), indicating the mitogenic action of LPA in these cells.[5] In addition, BMP22 inhibited MDA-MB-231 cell invasion across a Matrigel layer in a dose-dependent manner (Figure 3D) and across an endothelial cell monolayer in response to exogenous LPC plus recombinant ATX (Figure 3E). Taken together, these results indicate that blockade of ATX with BMP22 is highly potent in reducing LPA-dependent invasion of breast cancer cell lines.

ATX interaction with tumor cells requires functionally active integrin

ATX binds to activated $\alpha_{IIb}\beta_3$ integrin on blood platelets.[23] Association of β_3 with α_V subunits form the integrin $\alpha_V\beta_3$, which acts as a cell surface receptor for matrix proteins containing the RGD sequence motif that includes FN and OPN.[26] Activated integrin $\alpha_V\beta_3$ is known for its controlling role in cancer metastasis dissemination.[26] Hence, we tested the hypothesis that ATX bound to integrin $\alpha_V\beta_3$ expressed by tumor cells could control metastatic dissemination. We applied the previously established stable clones of CHO-dhfr$^+$ cells expressing either a functionally inactive (CHO-β_3Δ744) or active form of human integrin β_3 (CHO-β_3WT[14,15]; Figure 4A). Adhesion of CHO-β_3WT cells to ATX was significantly higher than that observed in parental CHO-dhfr$^+$ and CHO-β_3Δ744 cells (Figure 4B). Binding of CHO-β_3WT cells to increasing amounts of ATX became saturated at 200 ng (Figure 4C) and was completely inhibited when the cells were preincubated with the LM609 antibody (Figure 4D). In our experiments, adhesion of CHO-β_3WT cells to a series of ATX mutants harboring a single amino acid substitution or complete mutation of the RGD sequence was not significantly different from that seen in WT-ATX (supplemental Figure 1), and is in agreement with previously reported ATX crystal structure[27] and with the interference in cell adhesion of mutations in amino acid E109 and H117 in the somatomedin B2 domain of ATX.[23]

Because ATX is a secreted protein,[28] we examined its interaction with integrin $\alpha_V\beta_3$ in vitro. We performed coimmunoprecipitation studies using the LM609 antibody, with cell lysates obtained from CHO-β_3WT/ATX and CHO-dhfr$^+$/ATX cells, ATX coimmunoprecipitated with integrin $\alpha_V\beta_3$ in CHO-β_3WT/ATX cells but not in CHO-dhfr$^+$/ATX cells, which lack integrin $\alpha_V\beta_3$ (Figure 4E), confirming the physical interaction between ATX and integrin $\alpha_V\beta_3$. Moreover, adhesion of CHO-β_3WT cells to ATX-coated surfaces was dose-dependently competed by preincubation with soluble ATX (Figure 4F-G). Similarly, preincubation of CHO-β_3WT cells with the soluble catalytically-inactive (CI) ATX-T209A mutant inhibited cell adhesion to ATX (Figure 4G). These results indicate that soluble

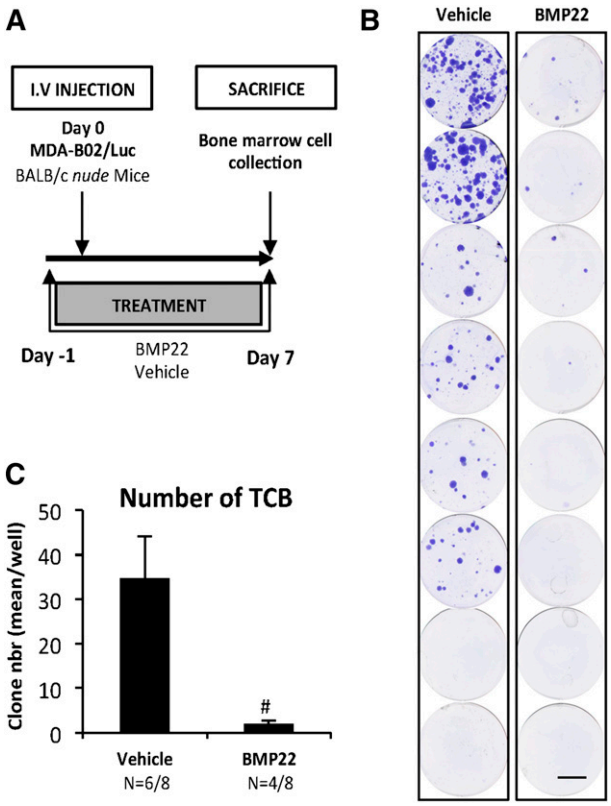

Figure 5. NT-ATX/lysoPLD controls early steps of tumor cell bone colonization. (A) Mice were injected IV with MDA-B02/luc cells and treated with BMP22 (1 mg/kg/day, i.p.) or vehicle from day 1 to day 8. (B) Bone marrow cells were collected and cultured for 2 weeks in the presence of puromycin (1 μg/mL). Colonies corresponding to tumor cells that colonized the bone (TCB) were fixed and stained with 20% methanol-crystal violet (v/v) (scale bar: 1 cm). (C) TCB colonies were counted. Results are expressed as mean of TCB (± SEM). Statistical analysis was performed using the nonparametric Mann-Whitney *U* test ($^{\#}P < .05$; vs vehicle-treated animals).

WT-ATX and CI-ATX-T209A compete with surface-bound WT-ATX for binding to integrin $\alpha_V\beta_3$.

To address the functional importance of ATX binding to the cell surface, via the integrin αVβ3, in the effect of platelet-derived ATX, we carried out proliferation assays using CHO-β3WT and CHO-β3-Δ744 cells expressing a functionally active and inactive form of this integrin, respectively. Proliferations of CHO-β3WT and CHO-β3Δ744 cells in presence of LPA were not statistically different (Figure 4H). Both cell lines did not respond to LPC alone, but had increased proliferation in presence of both LPC and recombinant ATX (Figure 4H). Under this condition, CHO-β3WT cells proliferated at a higher rate than CHO-β3Δ744 cells. This indicates that expression of a functional integrin αVβ3 but not its inactive mutant, provides a selective advantage for utilization of LPC in an ATX-mediated mechanism.

We also examined the binding of ATX to integrin $\alpha_V\beta_3$ using a series of human cancer cell lines from breast (MDA-BO2, ZR-7-51, and MCF7), prostate (DU145 and PC3), and osteosarcoma (MG-63). Expression levels of integrin $\alpha_V\beta_3$ were quantified by flow cytometry using the LM609 antibody (supplemental Figure 2A). High $\alpha_V\beta_3$-expressing cells (MG-63, DU145, and PC3 cells) had a significantly higher capacity than low $\alpha_V\beta_3$-expressing cells for adhering to ATX (supplemental Figure 2B-C). Likewise, MDA-BO2 cells, which had the highest levels of $\alpha_V\beta_3$ expression among all the breast cancer cell lines tested, also had the highest capacity for adhering to ATX (supplemental Figure 2B-C).

Altogether, these results demonstrate that ATX interacts physically with integrin $\alpha_V\beta_3$ expressed in cancer cells and that binding requires a functionally active integrin $\alpha_V\beta_3$, which impacts on tumor cell behavior.

NT-ATX controls the progression of osteolytic bone metastases of breast cancer

Although devoid of ATX, MDA-BO2/Luc cells produce extensive osteolytic bone metastases when injected into BALB/c nude mice.[17] At the bone metastatic site, LPA activates tumoral LPA_1, thereby inducing tumor cell proliferation and secretion of pro-osteoclastic cytokines (IL-6, IL-8, and GM-CSF).[8] Extending these earlier observations, in this study, we show that exogenous ATX induces the expression of IL-6 by MDA-B02/Luc cells only in the presence of LPC. Furthermore, this response is significantly inhibited by BMP22, indicating that LPA production is required for IL-6 secretion (supplemental Figure 3A). Next, we examined the effect of systemic BMP22 treatment on the progression of established osteolytic bone metastases of MDA-B02/Luc-inoculated BALB/C nude mice (supplemental Figure 3B). Daily treatment of the animals with BMP22 significantly reduced the osteolytic lesion areas by 39% ($P < .05$; supplemental Figure 3C). In agreement with a decrease in bone destruction and as a consequence of diminished secretion of pro-osteoclastic cytokines, BMP22 also reduced the number of osteoclasts at the tumor/bone interface by 22% ($P < .05$; supplemental Figure 3D). These results demonstrate that NT-ATX contributes to the progression of bone metastases through its lysoPLD activity.

NT-ATX controls early bone colonization of breast cancer cells

We next analyzed the role of NT-ATX during the early period of bone colonization by cancer cells (Figure 5A). Mice were injected with MDA-BO2/Luc cells, and tumor cells that colonized the bone marrow cavity (TCB) were collected 7 days postcell injection and expanded in vitro for 2 weeks. We found that the number of TCB clones was lower in the group of animals treated with BMP22 compared with vehicle-treated controls (94%) ($P < .001$; Figure 5B-C).

CI ATX-T209A prevents early bone colonization by breast cancer cells

We showed in Figure 4G that CI-ATX-T209A competed with WT-ATX for binding to integrin $\alpha_v\beta_3$ on the surface of cancer cells in vitro (Figure 4G). We hypothesized that administration of exogenous CI-ATX-T209A might potentially reduce bone colonization mediated by NT-ATX in vivo. To evaluate this hypothesis, we first generated CHO-$dhfr^+$ cells that stably express either WT-ATX (CHO/ATX) or CI-ATX (CHO/ATX-T209A). These cell lines expressed and secreted similar amounts of WT-ATX or CI-ATX-T209A protein (Figure 6A). Using ATX-Red dye and fluorescent imaging, we confirmed that high lysoPLD activity was detected only in the conditioned medium of CHO/ATX cells, which was effectively inhibited in the presence of BMP22 (Figure 6B). Next, BALB/c nude mice were injected with MDA-BO2/Luc cells and treated daily for 7 days with conditioned medium collected either from parental CHO-$dhfr^+$, CHO/ATX, or CHO/ATX-T209A cells. We found that the number of bone-derived colonies in the group of mice treated with CHO/ATX conditioned medium was not significantly lower compared with the group treated with conditioned medium from the parental CHO cells (Figure 6C). Intriguingly, treatment of animals with CHO/ATX-T209A cell medium significantly decreased by 66% ($P < .001$), the number of TCB compared with the

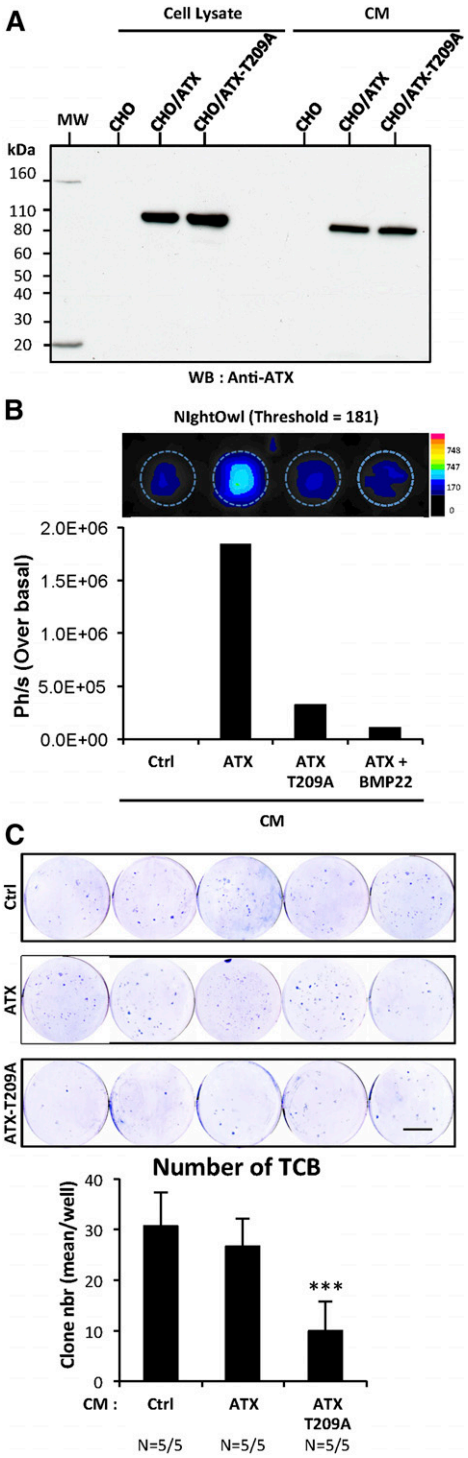

Figure 6. Inhibition of early steps of tumor cell bone colonization by circulating inactive ATX. (A) Detection of functionally active ATX and lysoPLD-deficient ATX-T209A expression in cell lysates and in conditioned media (CM) of CHO-dhfr$^+$/ATX and CHO-dhfr$^+$/ATX-T209A cells by immunoblotting using an anti-lysoPLD polyclonal antibody. (B) LysoPLD activity was quantified in cell culture CM in the presence or absence of BMP22 by fluorescence imaging on NightOwl using the ATX-Red compound (1 μM). Data are expressed as photon per second (Ph/s) over basal. Ctrl corresponds to parental CHO-dhfr$^+$ cells. (C) BALB/c nude mice were treated with CM (300 μL/twice daily, i.p.) collected from transfected parental CHO-dhfr$^+$ cells (Ctrl) or transfectants CHO-dhfr$^+$/ATX (ATX) and CHO-dhfr$^+$/ATX-T209A (ATX-T209A) cells 1 day before and the next 8 days after MDA-B02/luc cells injection (scale bar: 1 cm). Bone marrow cells were collected, cultured, and stained as described in Figure 5B (scale bar: 1 cm). (C) TCB colonies were counted. Results are expressed as mean of TCB (± SEM). Statistical analysis was performed using the nonparametric Mann-Whitney *U* test (***$P < 0.05$; vs vehicle-treated animals).

other groups. This result indicates that the administration of exogenous CI-ATX-T209A interferes with WT NT-ATX during the early steps of bone colonization by breast cancer cells.

Discussion

ATX gene expression is upregulated in many different types of cancers.[10] However, expression of ATX transcripts in human biopsies of primary breast tumors does not predict metastasis recurrence or overall patient survival.[13] Here, we show that systemic treatment of mice with the ATX inhibitor BMP22 blocks early bone colonization of breast cancer cells that lack ATX expression. This observation provides evidence that NT-ATX controls breast cancer cell metastasis. Our results broaden the paradigm for the role of ATX in cancer invasion and metastasis by establishing that, in addition to the ATX expressed by tumor cells, the ATX generated in the circulation through the interaction of the carcinoma cells with platelets also plays an equally important role.

ATX present in blood[29] is a major factor in generating circulating LPA.[30,31] We showed previously that mice depleted of platelets have diminished levels of plasma LPA, which in turn, prevents the progression of breast cancer bone metastases.[5] We were unable to detect ATX mRNA in platelets and in MKs. Nevertheless, we detected ATX protein stored in the α-granules of resting human platelets. Proteins of non-MK origin are frequently found in α-granules due to the ability of platelets to endocytose them. For example, fibrinogen, albumin, and immunoglobulins have been detected in platelet α-granules.[22,32] Proteins of platelet and nonplatelet origin stored in α-granules are released upon activation, and eventually contribute to thrombus formation. Here, we show that blocking platelet degranulation using inhibitors of integrin $\alpha_{IIb}\beta_3$ inhibits the release of stored ATX.

Metastatic cells exhibit a procoagulant activity that is required for successful metastasis dissemination.[1-4] Interaction of tumor cells with platelets induces the production of multiple tumor-promoting factors.[33-35] We have shown previously that incubation of platelets with cancer cells in steering conditions induces platelet aggregation and LPA production.[5] In this study, we demonstrate that passive interaction between platelets and breast cancer cells also results in the generation of LPA, that in turn promotes tumor cell proliferation. The antiaggregation interventions we tested, including RGDS peptide, ReoPro, apyrase, and clopidogrel, and the $LPA_{1/3}$ receptor antagonist Ki16425, efficiently blocked the mitogenic activity of platelet-derived LPA on tumor cells, indicating that LPA synthesis is coupled to platelet aggregation. Moreover, 2 unrelated inhibitors of lysoPLD activity (BMP22 and PF-8380) partially inhibited platelet-induced tumor cell proliferation, suggesting that ATX secreted from platelets, upon interaction with the tumor cells, is fully active and contributes to LPA production, albeit not exclusively.

Platelet activation is a major source of LPA production in mammals.[36] However, LPA released directly by platelets isolated from the plasma of noncancerous donors represents only a small fraction of LPA detectable in serum, indicating the role of a multistep enzymatic process leading to LPA accumulation during blood clotting.[37] We have shown that activated platelets secrete a novel lysophospholipase A1 (LYPLA-I/APT1) that generates a predominantly polyunsaturated species of LPC, that is in turn converted to LPA by circulating ATX during blood coagulation.[38] Our present results show that the nonspecific phospholipase A inhibitor palmostatin B, abolishes platelet-induced tumor cell proliferation, suggesting that the generation of bioactive LPA by activated platelets

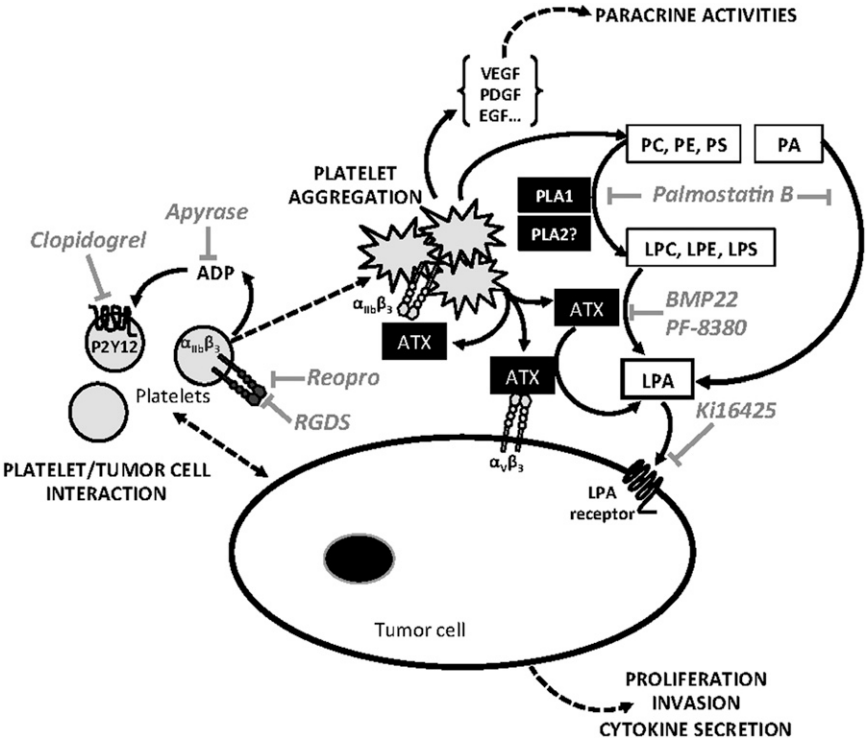

Figure 7. Schematic representation of LPA-dependent platelet-induced tumor cell metastasis. Tumor cell-induced platelet production of bioactive LPA (inhibitor: LPA receptor antagonist Ki16425) requires a first step of platelet aggregation that is prevented by selective inhibitors of $\alpha_{IIb}\beta_3$ integrin (RGDS, ReoPro), adenosine 5′-diphosphate activating pathway (Apyrase), and P2Y12 inhibitor (Clopidogrel). The second step requires the activation of phospholipases A1 and A2 (inhibitor: Palmostatin B) degrading membrane phospholipids among direct (phosphatidic acid) or indirect (phosphatidylcholine, phosphatidylserine, and phosphatidylethanolamine) precursors of LPA (LPC, lysophosphatidylserine, and lysophosphatidylethanolamine), that in turn are hydrolyzed by ATX/LysoPLD (ATX; lysoPLD inhibitors: BMP22 en PF-8380), released by activated platelets acting as free enzymes and/or bound to β_3 integrins ($\alpha_{IIb}\beta_3$ and $\alpha_V\beta_3$). LPE, lysophosphatidylethanolamine; LPS, lysophosphatidyserine; PA, phosphatidic acid; PC, phosphatidylcholine; PE, phosphatidylethanolamine; PLA1, phospholipase A1; PLA2, phospholipase A2; PS, phosphatidylserine.

requires the initial synthesis of sn-1 or sn-2 lysophospholipids, which are substrates for ATX.[37]

Binding of ATX to the integrin β_3 family members was discovered only recently.[23] Activated platelets (but not resting platelets) were shown to bind to ATX, indicating the necessity of integrin $\alpha_{IIb}\beta_3$ activation in this process.[23] Here, we found that expression of the dominant inactive integrin $\alpha_v\beta_3$-Δ744 or treatment of $\alpha_v\beta_3$-expressing cells with the anti-human $\alpha_v\beta_3$ antibody LM609 completely abolishes the binding of ATX to cells. Therefore, a fully active integrin $\alpha_v\beta_3$ is also required for tumor cell-induced LPA production. Moreover, we demonstrated that the level of integrin $\alpha_v\beta_3$ expression in osteosarcoma, prostate, and breast cancer cells shows direct correlation with ATX binding. Additionally, the CI-ATX-T209A mutant efficiently inhibited the binding of WT-ATX to integrin $\alpha_v\beta_3$, suggesting that these proteins compete for the same binding site in vitro. These results are in agreement with previous reports concerning multiple point mutations in the somatomedin B2 domain of ATX that failed to affect the catalytic site but impaired ATX binding to integrins.[23] Thus, competition for the integrin binding of ATX may have potential therapeutic implications in the treatment of cancer metastasis. A proof-of-concept for such an experimental therapy is presented in our experiments in which treatment of mice with CI-ATX-T209A conditioned medium inhibited early bone colonization of MDA-B02/Luc breast cancer cells. Such a dominant negative action of CI-ATX-T209A was also described previously in the immune system where CI-ATX-T209A prevented the entry of $CD4^+$ T-lymphocytes into secondary lymphoid organs.[39] A recent report also demonstrated cooperative action between exogenous ATX and integrins in directional cell migration, where binding of ATX to integrin enabled the uptake and subsequent redistribution of ATX to the leading edge of migrating cells.[40] Nonactivated platelets from Glanzmann's thrombasthenia patients lacking both integrins $\alpha_{IIb}\beta_3$ and $\alpha_V\beta_3$ revealed the role of these 2 integrins in importing fibrinogen into α-granules.[22] The binding of ATX to integrins $\alpha_{IIb}\beta_3$ and $\alpha_V\beta_3$ may represent a similar mechanism for the uptake of ATX from plasma into the α-granules. Fulkerson et al[23] showed that higher LPA production associated with CHO-$\alpha_{IIb}\beta_3$ cells incubated with exogenous ATX and LPC than that of parental CHO cells. Under these conditions, LPA production was dose-dependently inhibited by the integrin-blocking antibody 7E3, demonstrating the binding requirement of ATX to integrin $\alpha_{IIb}\beta_3$ for LPA production. ATX is a secreted protein and quantification of its lysoPLD activity in biological fluids is well documented. Thus, data presented in the literature firmly establishes that ATX can generate LPA regardless of whether they bound to integrins or in solution. Altogether, these studies suggest that cellular uptake, storage, and release of integrin-bound ATX may represent a general mechanism, even in cells that do not express ATX, providing localized production of LPA in close proximity to its cell surface receptors.

In conclusion, our results demonstrate that NT-ATX has an important epigenetic control over breast cancer cell metastasis. Moreover, NT-ATX stored in α-granules of resting platelets is secreted as a biologically active lysoPLD upon tumor cell-induced platelet aggregation. Our study provides a new framework for the mechanism by which platelets contribute to the LPA-dependent metastasis of breast cancer cells (Figure 7), and demonstrates the therapeutic potential of targeting NT-ATX in the prevention of metastasis in breast cancer patients.

Acknowledgments

The authors thank Dr J. Aoki from the University of Tohoku (Japan) for providing 4F1 monoclonal antibody, Dr C. Paillet from the Hospices Civils de Lyon (France) for providing ReoPro Abciximab, Dr C. Testa from Echelon Biosciences Incorporated (Salt Lake City, UT) for providing ATX-Red AR-2, and Jin Emerson-Cobb for editorial assistance. The authors acknowledge Elisabeth Errazuriz's

expert technical support with electronic microscopy (SFR Lyon Est, Lyon, France).

This work was supported by grants from the Institut National de la Santé et de la Recherche Médicale and the University of Lyon (O.P. and P.C.), the Comité Départemental de la Loire de la Ligue Contre le Cancer (O.P.), L'Association pour la Recherche sur le Cancer, ARC (O.P.), the National Cancer Institute at the National Institutes of Health (CA 092160) (G.J.T.), and the Harriet Van Vleet endowment (G.J.T.). R.L. was the recipient of a fellowship from the Ligue Nationale contre le Cancer. D.S. was the recipient of a fellowship from the Seventh Framework Programme (FP7/2007-2013) under agreement No. 264817-BONE-NET.

Authorship

Contribution: R.L. designed and performed cell-binding assays, conducted purifications of recombinant ATX and platelet-induced tumor cell proliferation assays, and contributed to the writing of the manuscript; S.-C.L. designed and conducted experiments for characterization of effects of BMP22 in cellular models and contributed to the writing of the manuscript; M.D. designed and performed site-directed mutagenesis and clone characterizations; J.-C.B. conducted human blood platelet isolation and electronic microscopy analyses; D.D.N. designed and performed LPA quantifications; R.P. synthesized BMP22; D.M. designed BMP22 and oversaw the synthesis and quality control; D.S. performed qRT-PCR and western blotting experiments; J.R. conducted murine cancer cell metastases experiments and bone tissue section analyses; P.C. contributed to the writing of the manuscript; and O.P. and G.J.T. were responsible for oversight of the project and preparation of the final manuscript.

Conflict-of-interest disclosure: The authors declare no competing financial interests.

Correspondence: Olivier Peyruchaud, INSERM U1033, Faculté de Médecine Lyon Est, Rue Guillaume Paradin, 69372 Lyon cedex 08, France; e-mail: olivier.peyruchaud@inserm.fr.

References

1. Gasic GJ, Gasic TB, Stewart CC. Antimetastatic effects associated with platelet reduction. *Proc Natl Acad Sci USA.* 1968;61(1):46-52.
2. Gasic GJ, Gasic TB, Galanti N, Johnson T, Murphy S. Platelet-tumor-cell interactions in mice. The role of platelets in the spread of malignant disease. *Int J Cancer.* 1973;11(3):704-718.
3. Karpatkin S, Pearlstein E, Ambrogio C, Coller BS. Role of adhesive proteins in platelet tumor interaction in vitro and metastasis formation in vivo. *J Clin Invest.* 1988;81(4):1012-1019.
4. Camerer E, Qazi AA, Duong DN, Cornelissen I, Advincula R, Coughlin SR. Platelets, protease-activated receptors, and fibrinogen in hematogenous metastasis. *Blood.* 2004;104(2): 397-401.
5. Boucharaba A, Serre C-M, Grès S, et al. Platelet-derived lysophosphatidic acid supports the progression of osteolytic bone metastases in breast cancer. *J Clin Invest.* 2004;114(12): 1714-1725.
6. Moolenaar WH, Hla T. SnapShot: bioactive lysophospholipids. *Cell.* 2012;148(1-2):378.
7. Mills GB, Moolenaar WH. The emerging role of lysophosphatidic acid in cancer. *Nat Rev Cancer.* 2003;3(8):582-591.
8. Boucharaba A, Serre CM, Guglielmi J, Bordet JC, Clézardin P, Peyruchaud O. The type 1 lysophosphatidic acid receptor is a target for therapy in bone metastases. *Proc Natl Acad Sci USA.* 2006;103(25):9643-9648.
9. Stracke ML, Krutzsch HC, Unsworth EJ, et al. Identification, purification, and partial sequence analysis of autotaxin, a novel motility-stimulating protein. *J Biol Chem.* 1992;267(4):2524-2529.
10. Umezu-Goto M, Kishi Y, Taira A, et al. Autotaxin has lysophospholipase D activity leading to tumor cell growth and motility by lysophosphatidic acid production. *J Cell Biol.* 2002;158(2):227-233.
11. Brindley DN, Lin FT, Tigyi GJ. Role of the autotaxin-lysophosphatidate axis in cancer resistance to chemotherapy and radiotherapy. *Biochim Biophys Acta.* 2013;1831(1):74-85.
12. Liu S, Umezu-Goto M, Murph M, et al. Expression of autotaxin and lysophosphatidic acid receptors increases mammary tumorigenesis, invasion, and metastases. *Cancer Cell.* 2009;15(6):539-550.
13. David M, Wannecq E, Descotes F, et al. Cancer cell expression of autotaxin controls bone metastasis formation in mouse through lysophosphatidic acid-dependent activation of osteoclasts. *PLoS ONE.* 2010;5(3):e9741.
14. Schaffner-Reckinger E, Gouon V, Melchior C, Plançon S, Kieffer N. Distinct involvement of beta3 integrin cytoplasmic domain tyrosine residues 747 and 759 in integrin-mediated cytoskeletal assembly and phosphotyrosine signaling. *J Biol Chem.* 1998;273(20): 12623-12632.
15. Pécheur I, Peyruchaud O, Serre CM, et al. Integrin alpha(v)beta3 expression confers on tumor cells a greater propensity to metastasize to bone. *FASEB J.* 2002;16(10):1266-1268.
16. Peyruchaud O, Winding B, Pécheur I, Serre CM, Delmas P, Clézardin P. Early detection of bone metastases in a murine model using fluorescent human breast cancer cells: application to the use of the bisphosphonate zoledronic acid in the treatment of osteolytic lesions. *J Bone Miner Res.* 2001;16(11):2027-2034.
17. Peyruchaud O, Serre C-M, NicAmhlaoibh R, Fournier P, Clezardin P. Angiostatin inhibits bone metastasis formation in nude mice through a direct anti-osteoclastic activity. *J Biol Chem.* 2003;278(46):45826-45832.
18. Kehlen A, Englert N, Seifert A, et al. Expression, regulation and function of autotaxin in thyroid carcinomas. *Int J Cancer.* 2004;109(6):833-838.
19. Gupte R, Patil R, Liu J, et al. Benzyl and naphthalene methylphosphonic acid inhibitors of autotaxin with anti-invasive and anti-metastatic activity. *ChemMedChem.* 2011;6(5):922-935.
20. Fells JI, Lee SC, Fujiwara Y, et al. Hits of a high-throughput screen identify the hydrophobic pocket of autotaxin/lysophospholipase D as an inhibitory surface. *Mol Pharmacol.* 2013;84(3):415-424.
21. Chen Z, Hu M, Shivdasani RA. Expression analysis of primary mouse megakaryocyte differentiation and its application in identifying stage-specific molecular markers and a novel transcriptional target of NF-E2. *Blood.* 2007; 109(4):1451-1459.
22. Handagama P, Rappolee DA, Werb Z, Levin J, Bainton DF. Platelet alpha-granule fibrinogen, albumin, and immunoglobulin G are not synthesized by rat and mouse megakaryocytes. *J Clin Invest.* 1990;86(4):1364-1368.
23. Fulkerson Z, Wu T, Sunkara M, Kooi CV, Morris AJ, Smyth SS. Binding of autotaxin to integrins localizes lysophosphatidic acid production to platelets and mammalian cells. *J Biol Chem.* 2011;286(40):34654-34663.
24. Gierse J, Thorarensen A, Beltey K, et al. A novel autotaxin inhibitor reduces lysophosphatidic acid levels in plasma and the site of inflammation. *J Pharmacol Exp Ther.* 2010;334(1):310-317.
25. Benesch MG, Ko YM, McMullen TP, Brindley DN. Autotaxin in the crosshairs: taking aim at cancer and other inflammatory conditions. *FEBS Lett.* 2014;588(16):2712-2727.
26. Felding-Habermann B, O'Toole TE, Smith JW, et al. Integrin activation controls metastasis in human breast cancer. *Proc Natl Acad Sci USA.* 2001;98(4):1853-1858.
27. Hausmann J, Kamtekar S, Christodoulou E, et al. Structural basis of substrate discrimination and integrin binding by autotaxin. *Nat Struct Mol Biol.* 2011;18(2):198-204.
28. Perrakis A, Moolenaar WH. Autotaxin: structure-function and signaling. *J Lipid Res.* 2014;55(6): 1010-1018.
29. Tokumura A, Majima E, Kariya Y, et al. Identification of human plasma lysophospholipase D, a lysophosphatidic acid-producing enzyme, as autotaxin, a multifunctional phosphodiesterase. *J Biol Chem.* 2002;277(42):39436-39442.
30. van Meeteren LA, Ruurs P, Stortelers C, et al. Autotaxin, a secreted lysophospholipase D, is essential for blood vessel formation during development. *Mol Cell Biol.* 2006;26(13): 5015-5022.
31. Tanaka M, Okudaira S, Kishi Y, et al. Autotaxin stabilizes blood vessels and is required for embryonic vasculature by producing lysophosphatidic acid. *J Biol Chem.* 2006; 281(35):25822-25830.
32. Harrison P, Wilbourn B, Debili N, et al. Uptake of plasma fibrinogen into the alpha granules of human megakaryocytes and platelets. *J Clin Invest.* 1989;84(4):1320-1324.
33. Labelle M, Begum S, Hynes RO. Direct signaling between platelets and cancer cells induces an epithelial-mesenchymal-like transition and promotes metastasis. *Cancer Cell.* 2011;20(5): 576-590.
34. Gay LJ, Felding-Habermann B. Contribution of platelets to tumour metastasis. *Nat Rev Cancer.* 2011;11(2):123-134.

35. Schumacher D, Strilic B, Sivaraj KK, Wettschureck N, Offermanns S. Platelet-derived nucleotides promote tumor-cell transendothelial migration and metastasis via P2Y2 receptor. *Cancer Cell.* 2013;24(1):130-137.

36. Gerrard JM, Robinson P. Identification of the molecular species of lysophosphatidic acid produced when platelets are stimulated by thrombin. *Biochim Biophys Acta.* 1989;1001(3):282-285.

37. Aoki J, Taira A, Takanezawa Y, et al. Serum lysophosphatidic acid is produced through diverse phospholipase pathways. *J Biol Chem.* 2002; 277(50):48737-48744.

38. Bolen AL, Naren AP, Yarlagadda S, et al. The phospholipase A1 activity of lysophospholipase A-I links platelet activation to LPA production during blood coagulation. *J Lipid Res.* 2011;52(5): 958-970.

39. Kanda H, Newton R, Klein R, Morita Y, Gunn MD, Rosen SD. Autotaxin, an ectoenzyme that produces lysophosphatidic acid, promotes the entry of lymphocytes into secondary lymphoid organs. *Nat Immunol.* 2008;9(4):415-423.

40. Wu T, Kooi CV, Shah P, et al. Integrin-mediated cell surface recruitment of autotaxin promotes persistent directional cell migration. *FASEB J.* 2014;28(2):861-870.

blood

2014 124: 3141-3150
doi:10.1182/blood-2014-04-568683 originally published online October 2, 2014

Interaction of platelet-derived autotaxin with tumor integrin $\alpha_V\beta_3$ controls metastasis of breast cancer cells to bone

Raphael Leblanc, Sue-Chin Lee, Marion David, Jean-Claude Bordet, Derek D. Norman, Renukadevi Patil, Duane Miller, Debashish Sahay, Johnny Ribeiro, Philippe Clézardin, Gabor J. Tigyi and Olivier Peyruchaud

Blood (print ISSN 0006-4971, online ISSN 1528-0020), is published weekly by the American Society of Hematology, 2021 L St, NW, Suite 900, Washington DC 20036.